

LS Scienza dei Materiali - a.a. 2005/06

## Fisica delle Nanotecnologie – part 2

Version 4b, Oct 2005

Francesco Fuso, tel 0502214305, 0502214293 - fuso@df.unipi.it

<http://www.df.unipi.it/~fuso/dida>

# Confinamento quantico e trasporto elettronico in nanostrutture

20/10/2005 – 10-11.30 – room B

27/10/2005 – 16.30-18 – room T1

## What are we looking for...

We deal with particles (e.g., electrons) moving in nanosized structures

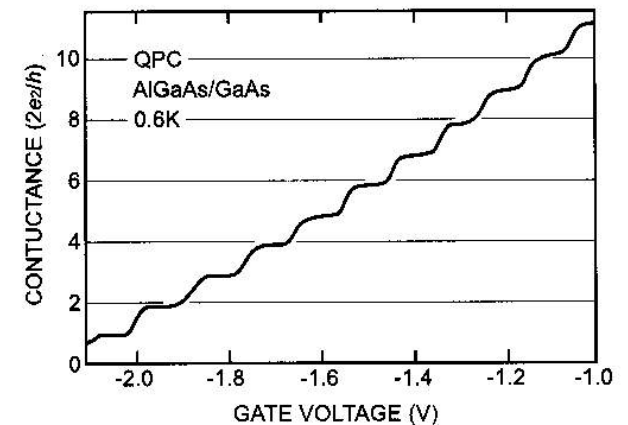
Quantum treatment of the particles implies wavefunctions (e.g., de Broglie,...)

If wavefunction extension  $\sim$  structure size, we expect **quantum confinement**

Known examples in **optics** ( $\lambda \sim$  hundreds of nm): optical cavity, optical fibers  
*Signatures of quantization*: radiation modes, supported standing waves, ...

In **transport properties**, dimensions are scaled down (we will see)

Expected signatures of quantization: non-ohmic behavior, tunneling effects, single electron, ...



**Expected advantages: miniaturization, speed, consumption, novel functions,...**

# Outlook

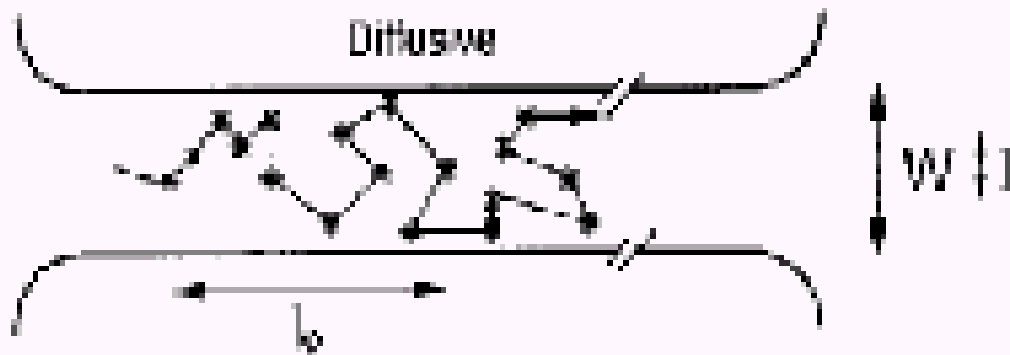
- Focus on “conventional” (silicon-based, inorganics) technology (we will mention other possibilities later on)
- Dimensionality of the structures and density of states for 3-D, 2-D, 1-D, 0-D structures (bulk, quantum wells, quantum wires, quantum dots)
- Electron transport and quantum confinement in **2-D structures in the presence of a magnetic field:**
  - High mobility 2-D electron gases at heterostructure interface;
  - Quantum electron in a magnetic field: Landau levels;
  - Quantum Hall Effect (integer, and a few words on the fractional effect);
  - von Klitzing quantum of resistance
- Electron transport and quantum confinement in **1-D structures without magnetic field:**
  - Landauer treatment and levels;
  - electron waveguides: “transverse modes”

## Conductivity in the classical (macroscopic) world

(Microscopic) Ohm's law:

$$\mathbf{J} = \sigma \mathbf{E} \rightarrow I = V/R \text{ with } R = l/(S \sigma)$$

In classical terms, resistance is a function of the dimensions (in bulk 3D materials, it is directly proportional to the length  $l$  and inversely proportional to the cross section  $S$ ):  **$R \sim (\text{typical width})^{(2\text{-dimensionality})}$**



Drude (either classical or quantum):  
**Diffusional motion of the electrons**

“Collisional” processes (material-dependent) rule the resistivity

**Dimensionality enters transport properties**

# Dimensionality and quantum confinement effects

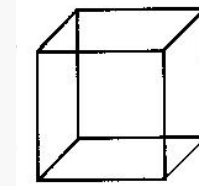
Quantum confinement effects expected whenever the **de Broglie wavelength** of the particle (i.e., the electron) approaches the typical size of the nanostructure

$$\lambda_{dB} = h/p \sim 7 \times 10^{-4} / v \text{ [m/s] in nm}$$

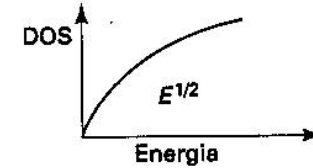
$$(v_{term} \sim 10^4 - 10^5 \text{ m/s}, v_F \sim 10^6 \text{ m/s})$$

$g(p) dp \propto L/h dp$	1-D
$S/h^2 2\pi p dp$	2-D
$V/h^3 4\pi p^2 dp$	3-D
↓	
$g(E) dE \propto dE$	1-D
$\sqrt{E} dE$	2-D
$\sqrt{E} dE$	3-D

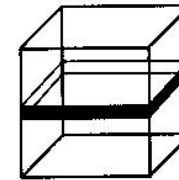
**DOS expression affected by dimensions**



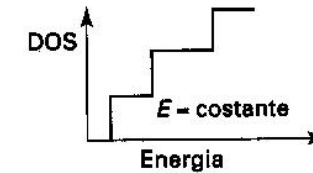
Bulk (3D)



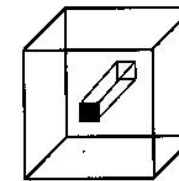
3DEG



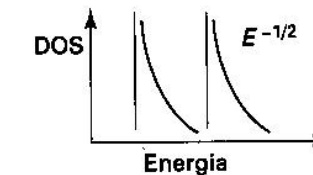
Quantum well (2D)



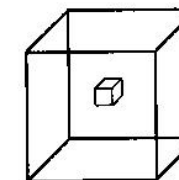
2DEG



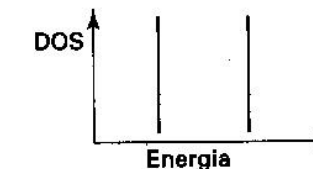
Quantum wire (1D)



1DEG



Quantum dot (0D)



0DEG

# Electron transport and quantum confinement

Transport properties depend on the dimensionality of the structures: **new and unexpected effects associated with quantum confinement** can arise

Quantum confinement is hard to be seen in 2DEG (2-dimension electron gases, e.g., conductive films)

Fully localized 0DEG structures (quantum dots) do require other processes for transport to occur (e.g., tunneling, as we will see in the next part)

Basically, 1DEG structures are well suited for investigating electron transport (**quantum wires**)

*Historically, the first observations are associated with the Quantum Hall Effect (QHE) in specific 2DEG structures with the presence of a static magnetic field*

# 2DEG in semiconducting heterostructures

## 1.1 Two-dimensional electron gas (2-DEG)

Recent work on mesoscopic conductors has largely been based on GaAs–AlGaAs heterojunctions where a thin two-dimensional conducting layer is formed at the interface between GaAs and AlGaAs. To understand why this layer is formed consider the conduction and valence band line-up in the  $z$ -direction when we first bring the layers in contact (Fig. 1.1.1a). The Fermi energy  $E_f$  in the widegap AlGaAs layer is higher than that in the narrowgap GaAs layer. Consequently electrons spill over from the

n-AlGaAs leaving behind positively charged donors. This space charge gives rise to an electrostatic potential that causes the bands to bend as shown. At equilibrium the Fermi energy is constant everywhere. The electron density is sharply peaked near the GaAs–AlGaAs interface (where the Fermi energy is inside the conduction band) forming a thin conducting layer which is usually referred to as the two-dimensional electron gas (2-DEG in short). The carrier concentration in a 2-DEG typically ranges from  $2 \times 10^{11}/\text{cm}^2$  to  $2 \times 10^{12}/\text{cm}^2$  and can be depleted by applying a negative voltage to a metallic gate deposited on the surface. The practical importance of this structure lies in its use as a field effect transistor [1.2, 1.3] which goes under a variety of names such as MODFET (Modulation Doped Field Effect Transistor) or HEMT (High Electron Mobility Transistor).

Note that this structure is similar to standard silicon MOSFETs, where the 2-DEG is formed in silicon instead of GaAs. The role of the wide-gap AlGaAs is played by a thermally grown oxide layer ( $\text{SiO}_2$ ). Indeed much of the pioneering work on the properties of two-dimensional conductors was performed using silicon MOSFETs [1.4]

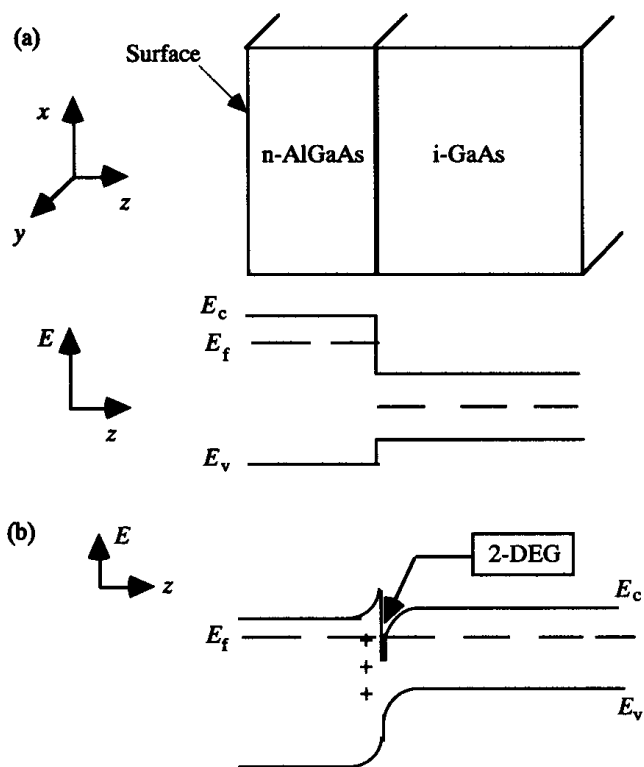


Fig. 1.1.1. Conduction and valence band line-up at a junction between an n-type AlGaAs and intrinsic GaAs, (a) before and (b) after charge transfer has taken place. Note that this is a cross-sectional view. Patterning (as shown in Fig. 0.3) is done on the surface ( $x$ - $y$  plane) using lithographic techniques.

After S.Datta, Electronic Transport in Mesoscopic Systems, Cambridge (1997)

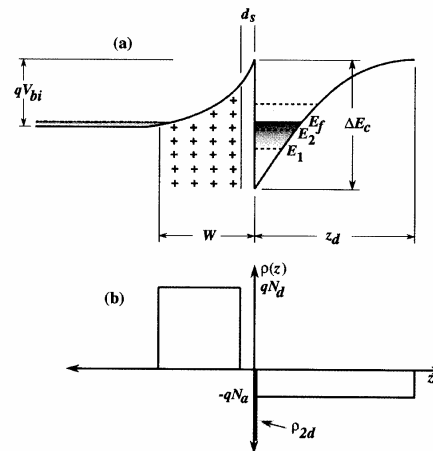


fig. 2.12. (a) Conduction band profile through a modulation-doped heterojunction system. (b) Charge density versus distance due to ionized donors and acceptors.

After Ferry and Goodnick, Transport in nanostructures, Cambridge (1997)

**“Band bending” at the interface produces localization in a 2DEG with typ. thickness 1-10 nm**

# Reminder on Fermi level in doped semiconductors I

## Fermi level and carrier density in doped semiconductors

### Carrier concentration in n-type semiconductors

We consider now extrinsic semiconductors, containing donor impurities, or acceptor impurities, or both, and we wish to study their influence on the Fermi level and the free carrier concentrations. We consider first the case of semiconductors in which only donor impurities are present (*n-type semiconductors*). The density  $N_d$  of donor impurities is supposed to be uniform in the sample, and the binding energy of the donor levels is  $\varepsilon_d$ . The schematic representation of the energy levels and occupancy at  $T = 0$  is given in Fig. 7a.

In intrinsic semiconductors we have seen that the Fermi level lies (basically) at the middle of the energy gap (see Eq. 6). Doping with donors (or acceptor) levels is the most common method to change in a controlled way the position of the Fermi level within the energy gap. The presence of donor levels shifts the Fermi level from the middle of the energy gap toward the edge of the conduction band. Let us in fact define the temperature

$$k_B T_d \equiv \varepsilon_d,$$

where  $T_d$  can be considered as the “ionization temperature” of the donor levels. If  $T \ll T_d$  we expect that practically all donor levels are occupied and thus the chemical potential must be located in the energy range  $E_d < \mu(T) < E_c$ . If  $T$  is comparable with  $T_d$  we expect that most donor levels are ionized and  $\mu(T)$  lies somewhat below the donor energy  $E_d$ , but still very near to the conduction band edge. At temperatures so high that the intrinsic carriers are much larger than the concentration of donor impurities, doping becomes uninfluential and we expect that the chemical potential approaches the middle of the bandgap. The chemical potential and the carrier concentration can be determined quantitatively from the knowledge of donor concentration,

G.Grosso and G.Pastori Parravicini,  
Solid State Physics (Academic, 2000)

density-of-states of the bulk crystal, and appropriate Fermi–Dirac statistics for band levels and donor levels.

The impurity states within the energy gap are described by localized wavefunctions; a donor level can thus be empty, or occupied by one electron of either spin, but not by two electrons (of opposite spin) because of the penalty in the electrostatic repulsion energy. Due to this, the probability  $P(E_d)$  that the level  $E_d$  is occupied by an electron of either spin is given by

$$P(E_d) = \frac{1}{(1/2) e^{(E_d - \mu)/k_B T} + 1}; \quad (19)$$

the above expression has been derived in Appendix III-C in the same way as the fundamental Fermi–Dirac statistics (1).

The chemical potential of the doped semiconductor is determined by enforcing the conservation of the total number of electrons as the temperature changes. In a semiconductor with  $N_d$  donor impurities per unit volume, the density  $n_0(T)$  of electrons in the conduction band must satisfy the relation

$$n_0(T) = N_d [1 - P(E_d)] + p_0(T) \quad (20)$$

where  $n_0$  and  $p_0$  are given by expressions (2). Eq. (20) is the straightforward generalization of Eq. (3); it states that the free electrons in the conduction bands are supplied by the thermal ionization of donor levels and by the thermal excitation of valence electrons. Eq. (20) can also be interpreted as an overall *charge neutrality condition* in the sample: the concentration  $n_0$  of negative charges equals the concentration of ionized donor impurities plus the concentration of holes.

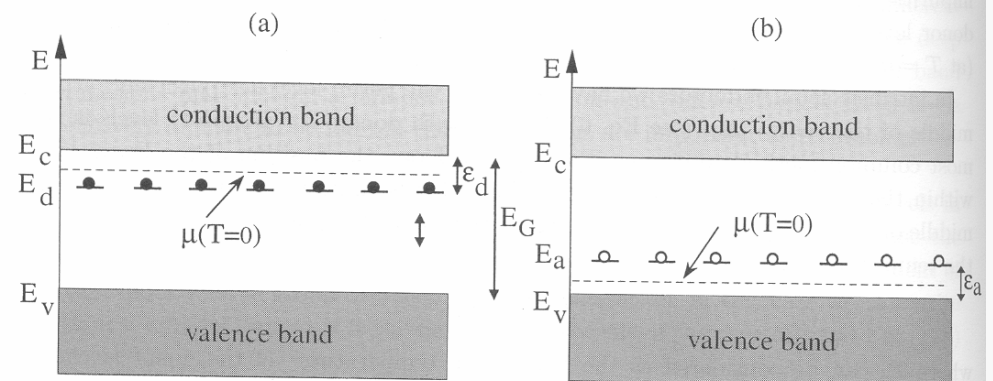


Fig. 7 (a) Schematic representation of the energy levels of a homogeneously doped n-type semiconductor at  $T = 0$  (in abscissa any arbitrary direction in the homogeneous material can be considered). Typical energy values are  $E_G = E_c - E_v \approx 1 \text{ eV}$  and  $\varepsilon_d = E_c - E_d \approx 10 \text{ meV}$ . The Fermi level at zero temperature lies at  $(1/2)(E_d + E_c)$ , which is the middle point between  $E_d$  and  $E_c$ . (b) Schematic representation of the energy levels of a homogeneously doped p-type semiconductor at  $T = 0$ ; typical values of  $\varepsilon_a = E_a - E_v$  are of the order of  $10 \text{ meV}$ . The Fermi level at zero temperature lies at  $(1/2)(E_v + E_a)$ , which is the middle point between  $E_v$  and  $E_a$ .

# Reminder on Fermi level in doped semiconductors II

Equation (20) can be solved (numerically) to obtain the Fermi level and hence the free carrier concentration. In the case the n-type semiconductor is non-degenerate (which is the ordinary situation, except for extremely high concentration of dopants), Eq. (20) can be simplified using Eqs. (5). We have:

$$N_c(T) e^{-(E_c - \mu)/k_B T} = N_d \frac{(1/2) e^{(E_d - \mu)/k_B T}}{(1/2) e^{(E_d - \mu)/k_B T} + 1} + N_v(T) e^{-(\mu - E_v)/k_B T}. \quad (21)$$

This is a third order algebraic expression in  $x = \exp(\mu/k_B T)$  that could be easily solved. We prefer to consider Eq. (21) in different regions of physical interest and handle it analytically.

(i) *Very low temperatures (or "freezing out region")*. Consider the semiconductor at very low temperatures  $T \ll T_d$ . In this temperature region we certainly have

$$E_d < \mu(T) < E_c.$$

Thus the second term in the right hand side of Eq. (21) can safely be neglected; furthermore the denominator in the first term in the right-hand side of Eq. (21) can be taken as unity. We have thus

$$N_c(T) e^{-(E_c - \mu)/k_B T} = \frac{1}{2} N_d e^{(E_d - \mu)/k_B T}; \quad (22a)$$

taking the logarithm of both members we obtain for the Fermi level

$$\mu(T) = \frac{1}{2} (E_d + E_c) + \frac{1}{2} k_B T \ln \frac{N_d}{2 N_c(T)}.$$

We can replace expression (22b) into equation (22a), and we obtain that the carrier density in the conduction band is

$$n_0(T) = N_c(T) e^{-(E_c - \mu)/k_B T} = \sqrt{N_c(T) \frac{N_d}{2}} e^{-\varepsilon_d/2 k_B T}.$$

Thus, the temperature dependence of the free electron carriers in n-type semiconductors at temperatures  $T \ll T_d$  has (approximately) the exponential form  $\exp(-\Delta/k_B T)$  where  $\Delta$  is half the binding energy of the donor levels. Notice that for high dopant concentration Eq. (22b) shows a tendency of  $\mu(T)$  to increase and possibly to invade the conduction band; in this situation we must consider directly the implicit equation (20) for determination of the chemical potential.

(ii) *Saturation region*. Consider the semiconductor in the temperature region  $T_d \ll T \ll E_G/k_B$ ; we expect that (almost) all donor levels are ionized, while the thermal excitation of valence electrons is still negligible. We have

$$n_0(T) = N_c(T) e^{-(E_c - \mu)/k_B T} \cong N_d; \quad (22c)$$

from the logarithm of both members, we have for the chemical potential

$$\mu(T) = E_c + k_B T \ln \frac{N_d}{N_c(T)}.$$

While the number  $n_0(T)$  of majority carriers is essentially constant and equal  $N_d$ , the number of minority carriers is obtained by considering the mass-action law (7). In the *saturation region*, characterized by all donor levels ionized, and at temperatures where

$n_i(T) \ll N_d$ , we have

$$n_0(T) \cong N_d \quad \text{and} \quad p_0(T) \cong \frac{n_i^2(T)}{N_d}. \quad (24c)$$

For instance, the intrinsic carrier concentration of silicon at room temperature is  $n_i(T) \approx 10^{10} \text{ cm}^{-3}$ . In n-type silicon with donor concentration  $N_d \approx 10^{14} \text{ cm}^{-3}$ , we have  $n_0 \approx 10^{14} \text{ cm}^{-3}$  and  $p_0 \approx 10^6 \text{ cm}^{-3}$ ; in the above situation there are eight orders of magnitude in the difference between the concentration of majority carriers and of minority carriers. Notice also that in silicon  $N_c(T) \approx 10^{19} \text{ cm}^{-3}$ ; the chemical potential (24b) remains near the conduction band edge, but safely below it, so that the non-degeneracy conditions (4) are justified. As another example, consider an n-type GaAs crystal at room temperature with  $n_i(T) \approx 10^7 \text{ cm}^{-3}$  and  $n_0 \approx N_d \approx 10^{14} \text{ cm}^{-3}$ ; in this case we have  $p_0 \approx 1 \text{ cm}^{-3}$ , a value fourteen orders of magnitude less than the majority carrier concentration.

(iii) *Intrinsic region*. If we increase further the temperature, the thermal excitation of valence electrons into the conduction band increases, and eventually the intrinsic situation is recovered. The temperature dependence of the density of free electron carriers in an n-type semiconductor is schematically summarized in Fig. 8.

Up to this point, impurities have been (tacitly) considered as isolated and independent; furthermore the doped semiconductor is assumed to remain non-degenerate, i.e. the Fermi level is several  $k_B T$  away from the band edges. As the concentration of dopants is increased new phenomena occur; for instance, the Fermi level may approach and invade the energy bands; the density-of-states of the semiconductor may be perturbed near the edges and a bandgap narrowing may result; the impurity levels may interact forming an impurity band, with effects on the conductivity of the sample; here, we do not enter in these and other interesting consequences of heavy doping in semiconductors.

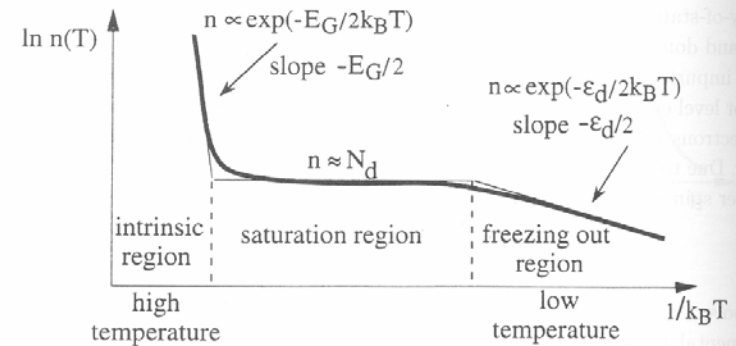


Fig. 8 Schematic variation of the electron concentration as a function of  $1/k_B T$  in an n-type semiconductor with  $N_d$  donor impurities per unit volume.

# High mobility in MODFET/HEMT structures

## Mobility

What makes the 2-DEG in GaAs very special is the extremely low scattering rates that have been achieved. The **mobility** (at low temperatures) provides a direct measure of the momentum relaxation time as limited by impurities and defects. Let us first briefly explain the meaning of mobility. In equilibrium the conduction electrons move around randomly not producing any current in any direction. An applied electric field  $\mathbf{E}$  gives them a drift velocity  $\mathbf{v}_d$  in the direction of the force  $e\mathbf{E}$  as shown in Fig. 1.1.2. To relate the drift velocity to the electric field we note that, at

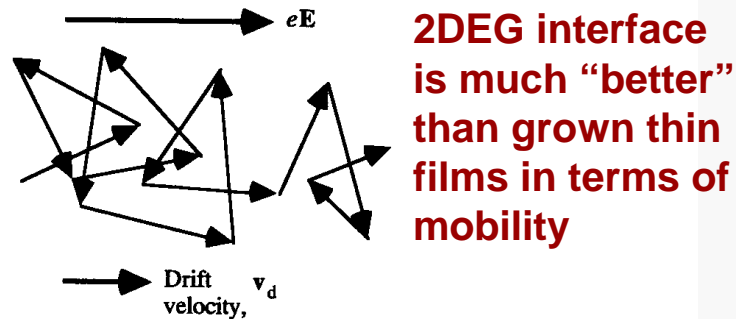


Fig. 1.1.2. In the presence of an electric field the electrons acquire a drift velocity superposed on their random motion.

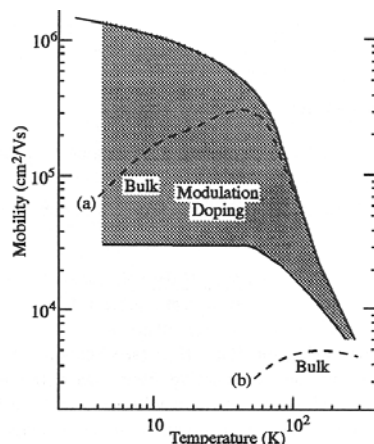


Fig. 1.1.3. Mobility vs. temperature in modulation-doped structures. Higher mobility (but lower carrier concentration) is obtained with thicker buffer layers. Also shown for comparison is the mobility in (a) high purity bulk GaAs and in (b) doped GaAs for use in FETs. Adapted with permission from Fig. 9 of T. J. Drummond, W. T. Masselink and H. Morkoc (1986). *Proc. IEEE*, 74, 779. © 1986 IEEE

**High "in-plane" mobility achieved (collisions negligible)**

steady-state, the rate at which the electrons receive momentum from the external field is exactly equal to the rate at which they lose momentum ( $\mathbf{p}$ ) due to scattering forces:

$$\left[ \frac{d\mathbf{p}}{dt} \right]_{\text{scattering}} = \left[ \frac{d\mathbf{p}}{dt} \right]_{\text{field}}$$

Hence, ( $\tau_m$ : momentum relaxation time)

$$\frac{m\mathbf{v}_d}{\tau_m} = e\mathbf{E} \Rightarrow \mathbf{v}_d = \frac{e\tau_m}{m} \mathbf{E}$$

The mobility is defined as the ratio of the drift velocity to the electric field:

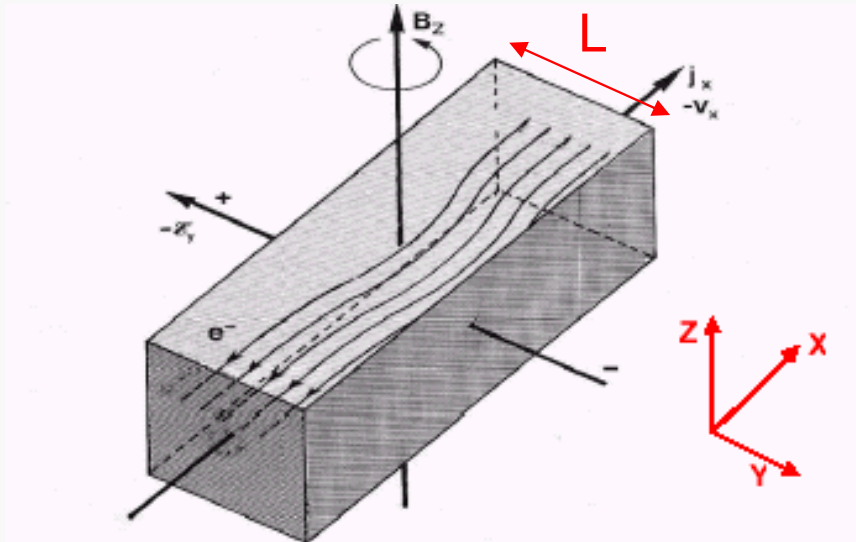
$$\mu = \left| \frac{v_d}{E} \right| = \frac{|e|\tau_m}{m} \quad (1.1.1)$$

Mobility measurement using the Hall effect (see Section 1.5) is a basic characterization tool for semiconducting films. Once the mobility is known, the momentum relaxation time is readily deduced from Eq.(1.1.1).

In bulk semiconductors as we go down from room temperature, the momentum relaxation time increases at first due to the suppression of phonon scattering. But it does not increase any further once the phonon scattering is small enough that impurity scattering becomes the dominant mechanism (see Fig. 1.1.3). With a donor concentration of  $10^{17}/\text{cm}^3$  the highest mobility is less than  $10^4 \text{ cm}^2/\text{V s}$ . Higher mobilities can be obtained with undoped samples but this is not very useful since there are very few conduction electrons.

In a 2-DEG, on the other hand, carrier concentrations of  $10^{12}/\text{cm}^2$  in a layer of thickness  $\sim 100 \text{ \AA}$  (equivalent bulk concentration of  $10^{18}/\text{cm}^3$ ) have been obtained with mobilities in excess of  $10^6 \text{ cm}^2/\text{V s}$  (the current record is almost an order of magnitude larger than what is shown in Fig. 1.1.3). The reason is the spatial separation between the donor atoms in the AlGaAs layer and the conduction electrons in the GaAs layer. This reduces the scattering cross-section due to the impurities, leading to weaker scattering. Often an extra buffer layer of undoped AlGaAs is introduced between the GaAs and the n-AlGaAs in order to increase the separation between the 2-DEG in the GaAs and the ionized donors in the AlGaAs. This reduces the scattering but it also reduces the carrier concentration.

# Classical Hall effect in a conductor



$$V_H = R_H I = v_d B L = \mu B L / e$$

Mobility can be measured (including the sign) by Hall experiments

**Classically, the Hall resistance is a continuous feature depending on the mobility**

A known current is sent along x

A known magnetic field (static and homogeneous) is applied along z

In a two-charge fluid model of the current, Lorentz force drives positive and negative charge along y, with a sign depending on the charge polarity

At equilibrium, charge separation occurs (along y)

-> an electric field exists

-> a potential difference can be measured across y direction

# Electron dynamics in a magnetic field (quantum)

Effetti quantistici: diventano importanti ad esempio quando la separazione dei livelli energetici quantizzati è paragonabile a energia del sistema, oppure quando la lunghezza d'onda di de Broglie  $\lambda_{dB} = h/p$  si avvicina ad una lunghezza caratteristica del sistema.

Nel QHE si ha quantizzazione dell'energia dovuta alla presenza di B, che produce effetti osservabili (anche per valori di campo *realistici*) grazie alle piccole dimensioni del sistema in una direzione.

## 0.1 Moto classico di un elettrone in presenza di B

Suppongo  $\mathbf{B} = B \hat{z}$ . Dalla forza di Lorentz

$$\mathbf{F}_{Lorentz} = -e\mathbf{v} \times \mathbf{B} \quad (1)$$

si ha:

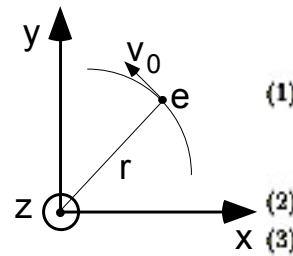
$$m\dot{v}_x = -ev_y B \quad (2)$$

$$m\dot{v}_y = ev_x B, \quad (3)$$

da cui (derivando e sostituendo):

$$m\ddot{v}_x = -\frac{e^2 B^2}{m} v_x. \quad (4)$$

Il moto lungo x ed y è oscillatorio con la pulsazione di ciclotrone  $\omega_c = eB/m$ . La combinazione dei moti lungo x ed y con opportune condizioni iniziali dà luogo ad un moto circolare con la stessa pulsazione e raggio arbitrario (purché  $\omega_c = v_0/r$ ). Se l'elettrone ha anche moto lungo z, la traiettoria è una spirale.



## 0.2 Trattazione quantistica

L'Hamiltoniana di un elettrone in presenza di B è (gauge di Lorentz)\*

$$\mathcal{H} = \frac{1}{2m} (\mathbf{p} - e\mathbf{A})^2, \quad (5)$$

con  $\mathbf{A}$  potenziale vettore ( $\nabla \times \mathbf{A} = \mathbf{B}$ ). Nel nostro caso conviene scegliere  $\mathbf{A} = (-By, 0, 0)$ , quindi si ha:

$$\mathcal{H} = \frac{1}{2m} ((p_x + eBy)^2 + p_y^2 + p_z^2). \quad (6)$$

Dato che non compare dipendenza esplicita né da x né da z,  $p_x$  e  $p_z$  sono costanti del moto, quindi la soluzione sarà del tipo  $\psi = \exp(ik_x x) \exp(ik_z z) \mathcal{F}(y)$ , con

$\mathcal{F}(y)$  funzione da determinare attraverso l'applicazione dell'eq. di Schrödinger (Eq. 6), che dà:

$$-\frac{\hbar^2}{2m} \frac{\partial^2 \mathcal{F}}{\partial y^2} + \frac{1}{2} m \omega_c^2 (y - y_0)^2 \mathcal{F} = E' \mathcal{F}, \quad (7)$$

con  $E'$  espressione opportuna di energia. Questa è l'equazione di un oscillatore armonico lungo y con pulsazione  $\omega_c$  e centro di oscillazione:

$$y_0 = -\frac{\hbar k_x}{eB}. \quad (8)$$

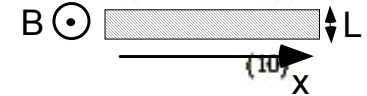
I livelli di energia sono quantizzati con autovalori:

$$E_{n,j} = E_{kin} + (n + \frac{1}{2}) \hbar \omega_c, \quad (9)$$

dove j è un numero quantico riferito all'energia cinetica  $E_{kin}$ . Si noti che i valori del quanto di energia sono generalmente bassi (meV o frazioni di meV) per campi magnetici usuali.

Se il sistema ha piccole dimensioni lungo y (supponiamo lo spessore sia L), allora deve essere  $|y_0| \leq L$ , da cui:

$$k_x < \frac{eBL}{\hbar} = \frac{\omega_c mL}{\hbar}.$$



Quindi, la bassa dimensionalità lungo y produce una limitazione sul valore di  $k_x$  (effetto di "mescolamento" delle direzioni spaziali tipico delle situazioni in cui si ha a che fare con un campo magnetico).

## 0.3 Densità degli stati e degenerazione

Nel caso unidimensionale, che qui si applica per tenere conto del confinamento spaziale lungo la direzione y, e di conseguenza del confinamento nello spazio k lungo la direzione x (vedi Eq. (10)), si ha che la densità degli stati (riferita solo alla direzione di quantizzazione) è:

$$g(k_x) dk_x = dk_x \frac{L}{2\pi}. \quad (11)$$

Considerando la sola direzione x, integrando si ottiene:

$$\int_0^k dk_x \frac{L}{2\pi} = \frac{eBL^2}{2\pi\hbar}, \quad (12)$$

dove si è tenuto conto della condizione Eq. (10). Dividendo l'espressione al membro di destra di Eq. (12) per  $L^2$  si ottiene in pratica una densità ( $n_s$ ) di portatori di carica per unità di superficie (reale), che vale quindi:

$$n_s = \frac{eB}{2\pi\hbar}. \quad (13)$$

\*  $\phi \rightarrow \phi + \frac{\partial \psi}{\partial t}, \quad \frac{1}{c^2} \frac{\partial \phi}{\partial t} + \nabla \cdot \mathbf{A} = 0.$   
 $\mathbf{A} \rightarrow \mathbf{A} - \nabla \psi,$

# Landau levels

D'altra parte, l'energia del portatore di carica si può scrivere

$$E = E_n + \frac{\hbar^2 k_x^2}{2m}, \quad (14)$$

dove rispetto alla Eq. (14) si è esplicitata la parte cinetica. Dalla Eq. (14) si ricava

$$dk_x = \frac{\sqrt{2m}}{2\hbar} \frac{1}{\sqrt{E - E_n}} dE \quad (15)$$

da cui

$$g(E) \propto \frac{1}{\sqrt{E - E_n}}, \quad (16)$$

densità degli stati tipica per un gas 1-DEG. In corrispondenza delle energie  $E_n$  la  $g(E)$  tende a divergere (livelli di Landau).

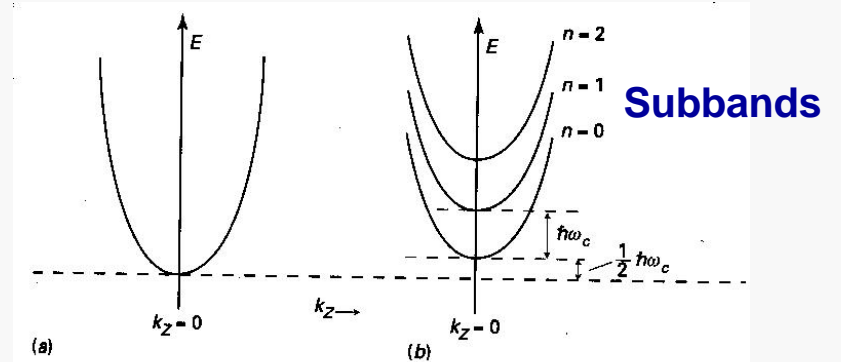


Figura 9.3

Schema di bande di energia in funzione di  $k_z$  in assenza (a) ed in presenza (b) di un campo magnetico  $\vec{B}$  applicato in direzione  $z$  (vedi eq. 9.52).

## 1D-like density of states

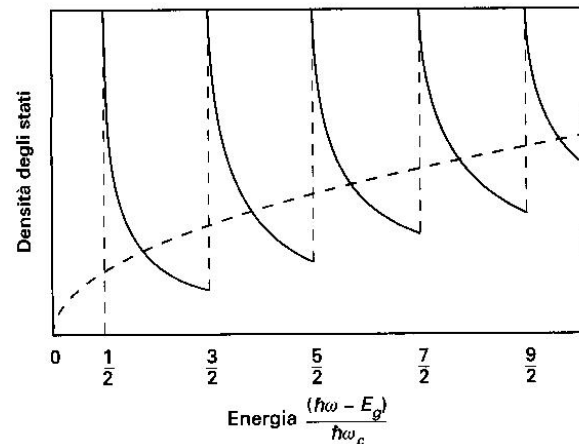


Figura 9.5

Densità di stati vicino al minimo di una banda in presenza di un campo magnetico costante: il caso  $B = 0$  è indicato con linea tratteggiata (vedi eq. 8.25) e il caso  $B \neq 0$  con linea continua (vedi eq. 9.58).

(Surface) density of states, i.e., carrier density, corresponding to each Landau level is  $eB/h$

For a given number of carriers (electrons), a **B value** exists so that *all* carriers are in the ground level

**The small thickness of the conductor combined with the presence of the magnetic field leads to a 1D-like behavior**

# QHE and von Klitzing quantum of resistance I

## 0.4 Quanto di resistenza di Von Klitzing

Considerando la forza di Lorentz come forza elettromotrice, nell'effetto Hall classico si ha che la differenza di potenziale  $V_H$  (in direzione  $y$ , cioè trasversa rispetto al moto delle cariche e al campo magnetico) è  $V_H = LBv$  e la corrente di portatori di carica è  $I = n_s v e L$ , con  $n_s$  densità superficiale di carica già introdotta. Dalla legge di Ohm si deduce una resistenza Hall  $R_H$ :

$$R_H = \frac{V_H}{I} = \frac{B}{n_s e} \quad (17)$$

Nel QHE, l'azione combinata del campo magnetico e del confinamento spaziale porta alla presenza dei livelli di Landau e alla loro degenerazione. Quando un livello di Landau (supponiamo il livello  $m$ ) è completamente occupato e il successivo è completamente vuoto, cioè  $m$  livelli di Landau sono pieni, ognuno con la degenerazione vista in precedenza, allora, secondo la Eq. (13), si avrà un numero di elettroni per unità di superficie pari a:

$$n = m \frac{eB}{h} \quad (18)$$

da cui deriva che la resistenza Hall si esprime come sottomultiplo del valore  $h/e^2$ , dipendente solo da costanti fondamentali:

$$R_H = \frac{1}{m} \frac{h}{e^2} \quad (19)$$

**Fine structure constant**

Questo risultato ha diverse conseguenze. In primo luogo stabilisce un valore quantizzato della resistenza (il cui valore è 25812.806 ohm). Occorre notare che nell'effetto Hall quantistico la quantizzazione della resistenza è conseguenza del confinamento spaziale, ma la sua osservazione è resa possibile dalla presenza del campo magnetico (e conseguente quantizzazione del moto dei portatori di carica). In condizioni ordinarie l'effetto di quantizzazione non è facilmente osservabile (e, in generale, si ricordi che la resistenza misurata può essere interpretata come un parallelo di tante resistenze). Inoltre esistono delle conseguenze notevoli dal punto di vista metrologico, legate alla precisione con cui si può eseguire la misura delle costanti fondamentali  $h$  e  $e^2$ . Dal punto di vista tecnologico, la conseguenza principale è comunque che la differenza di potenziale misurata non è lineare con la corrente, ma segue un tipico andamento a gradini. Per ragioni di tipo sperimentale, i sistemi in cui tradizionalmente si osserva QHE sono delle eterostrutture, ad esempio tipo GaAs/GaAsAl, in cui il confinamento spaziale è ottenuto in strati sottili (pozzi quantici).

Per completezza, occorre ricordare che accanto al QHE intero, scoperto da Von Klitzing (premio Nobel 1985), esiste un QHE frazionario, legato all'occupazione frazionaria dei livelli di Landau (Tsui and Stormer, premio Nobel 1998).

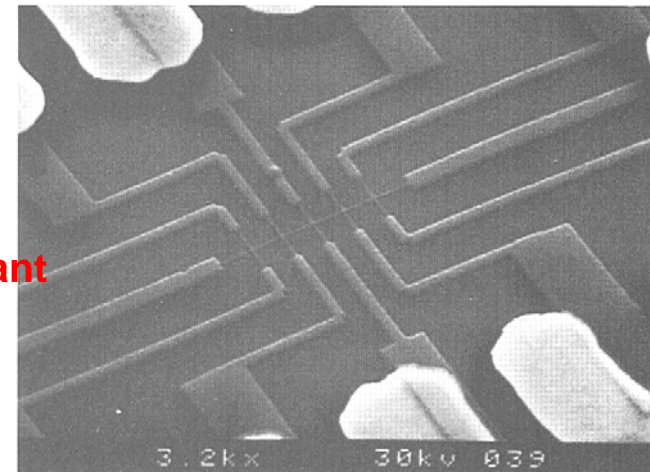
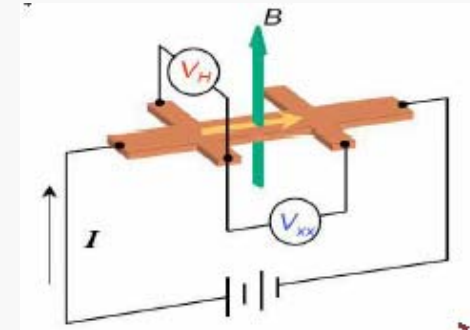


Fig. 0.3. Scanning electron micrograph of a long wire 75 nm wide patterned from a GaAs-AlGaAs heterojunction. Four-terminal Hall measurements are made using voltage probes placed along the wire  $\sim 2 \mu\text{m}$ . apart. Reproduced with permission from M. L. Roukes, A. Scherer, S. J. Allen, H. G. Craighead, R. M. Ruthen, E. D. Beebe and J. P. Harbison (1987), *Phys. Rev. Lett.* 59, 3011.

Measurements carried out at very low temperature in order to decrease (phonon) scattering

# QHE and von Klitzing quantum of resistance II

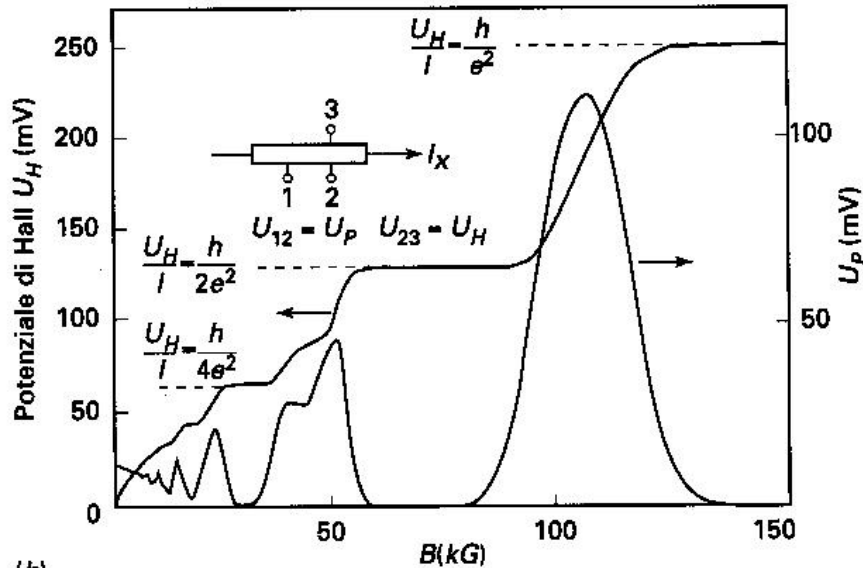
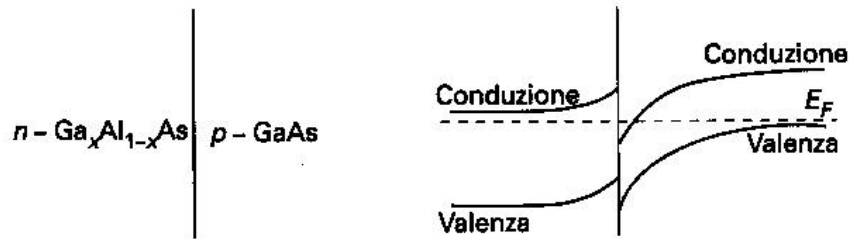
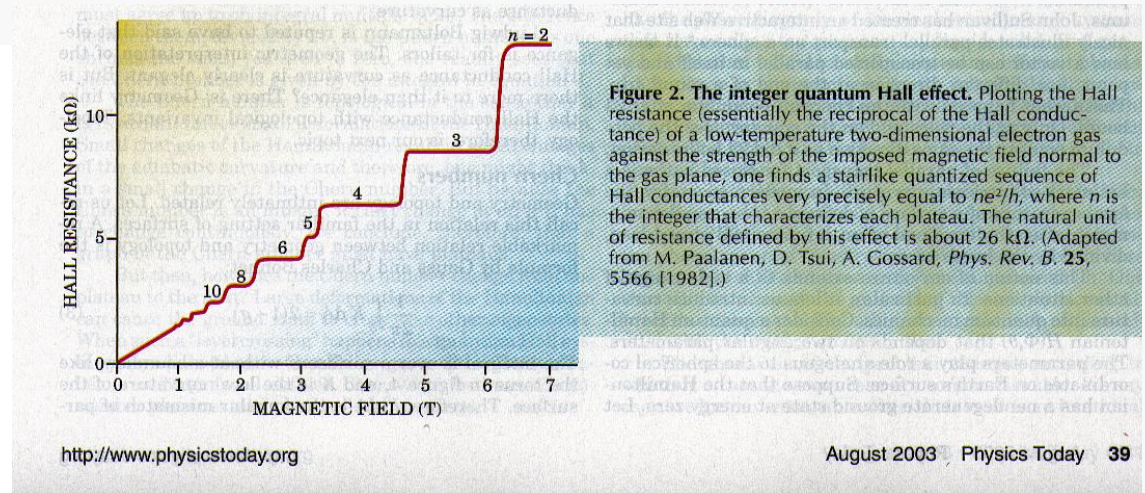


Figura 11.11

(a) Indicazione schematica della giunzione con campo elettrico, che produce stati con mobilità alla superficie della giunzione. (b) Misure di effetto Hall quantizzato, con i caratteristici gradini dove il potenziale di Hall è costante, e il potenziale nella direzione della corrente è nullo. (Da K. von Klitzing, Europhysics News 13, 2 (Aprile 1982)).



Resistance is quantized in units of  $R_{vk} \sim 25.8 \text{ Kohm}$

The quantum depends on the fine structure constant, i.e., on fundamental quantities (e, h)

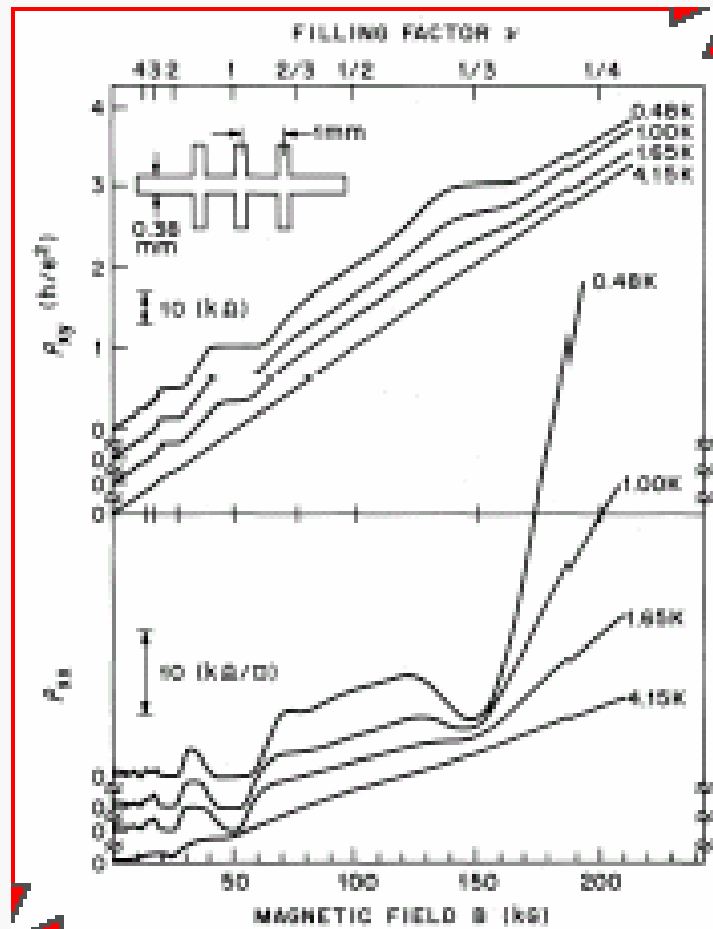
# A few words on fractional-QHE

1982 (Tsui, Stoermer, et al.): discovery of **Fractional-QHE**

$$R_H = \frac{p}{q} \frac{h}{e^2}$$

$$\nu = \frac{p}{2mp \pm 1}$$

Filling factor



Interpretation (Laughlin): many-body problem

The Hamiltonian should include terms accounting for interaction inter-electron and electron-ion (lattice)

A collective wavefunction (product of single electron wavefunction) should be used and the corresponding Landau levels identified

Degeneracy of the levels turns out to depend on the specific system considered

## Towards 1DEG

We have seen that 2DEG structures *with* magnetic field  $\mathbf{B}$  do exhibit quantized transport behavior (von Klitzing quantum of resistance)

Role of  $\mathbf{B}$ : mix up the directions so that 2DEG DOS behaves similar to 1DEG

If  $\mathbf{B} = 0$  no quantum effect is observed (the charge carriers can always find a “non confined” direction for their motion!)

**1DEG** structures (**quantum wires**) expected to show a signature of quantum confinement effects *without*  $\mathbf{B}$

From the **technological** point of view, a 1DEG is quite complicated to achieve in “conventional” electronics (inorganics), but it can be done

The simplest way, at least ideally, is based on the exploitation of either **linear conductive molecules** (organics) or **mesoscopic structures** (nanowires/nanotubes): we will see more!

# Examples of realization of 1-D nanostructures (conventional) I

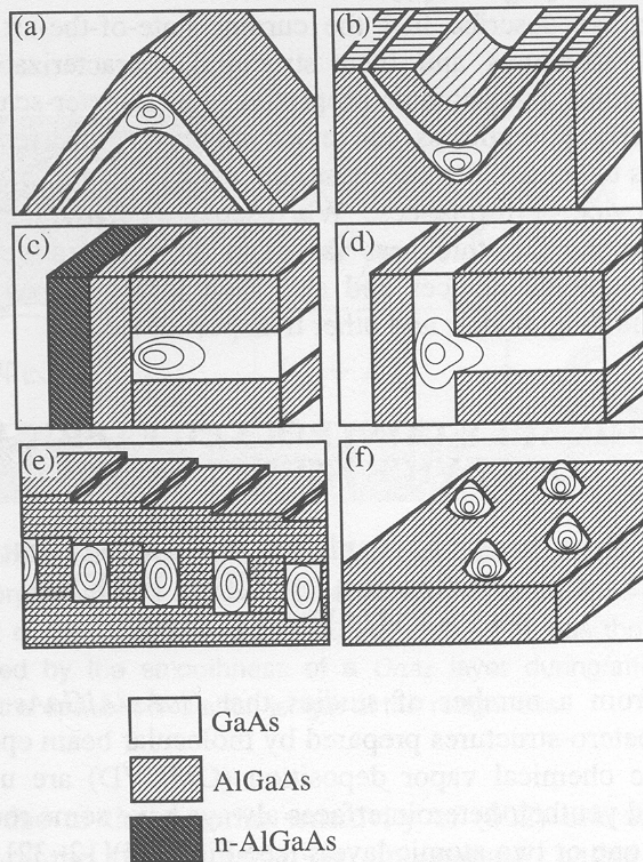


**FIGURE 3.** Examples of epitaxially grown QWRs and QBs. A ridge QWR (a), a groove QWR (b), a (field-induced) edge QWR (c), a (T-shaped) edge QWR (d), a tilted superlattice (TSL) (e), and a self-assembled QB structure (f). See section VI.B for their details and references.

Film growth with specific arrangements (e.g., onto specifically “cut” substrates)

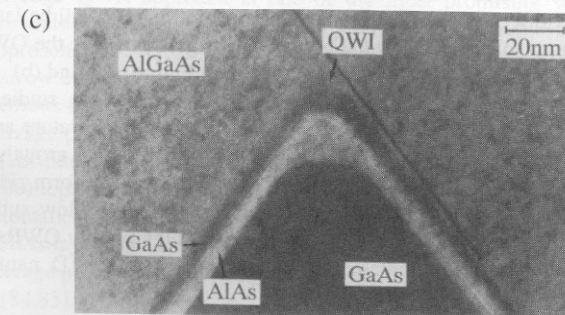
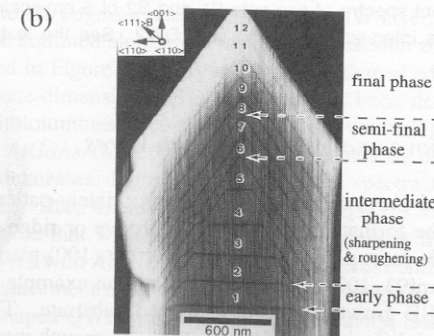
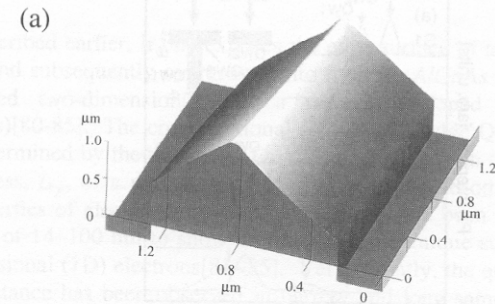


**FIGURE 20.** (a) An AFM image of an MBE grown *GaAs* ridge. (b) An SEM cross-sectional image of a *GaAs* ridge with thin *AlAs* marker layers. (c) A TEM image of a ridge quantum wire structure after Koshiba *et al.*[97]. (See color plate.)

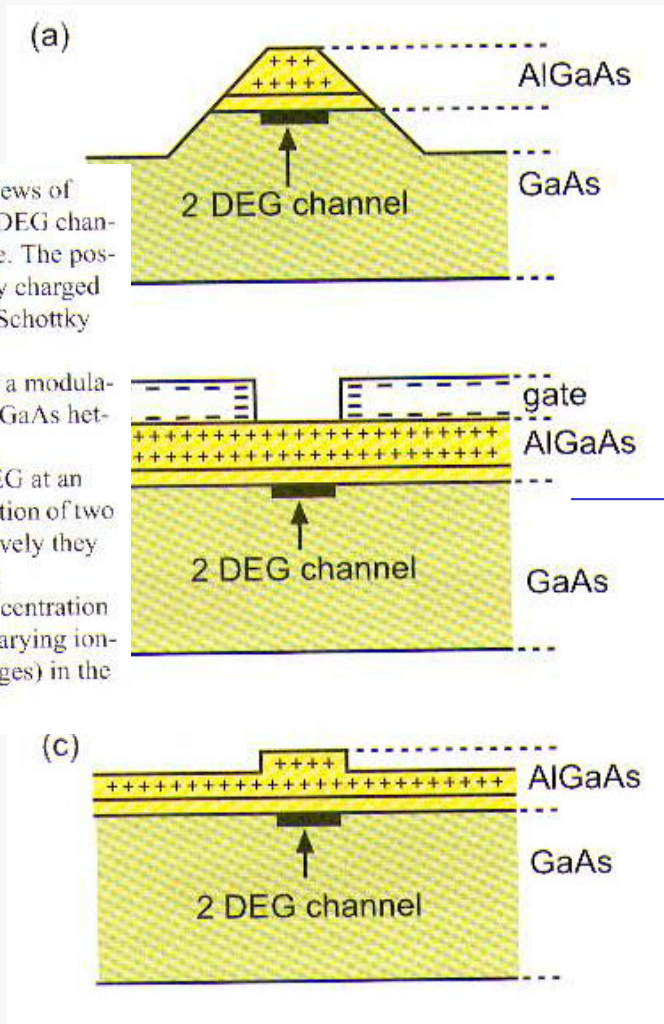
# Examples of realization of 1-D nanostructures (lithography) II

**Figure 16:** Schematic cross sectional views of three different ways to define narrow 2-DEG channels in an AlGaAs/GaAs heterostructure. The positively ionized donors and the negatively charged 2-DEG channel as well as the negative Schottky gate electrode (b) are indicated.

(a) Lithographically structured wire on a modulation doped (AlGaAs n-doped) AlGaAs/GaAs heterostructure.

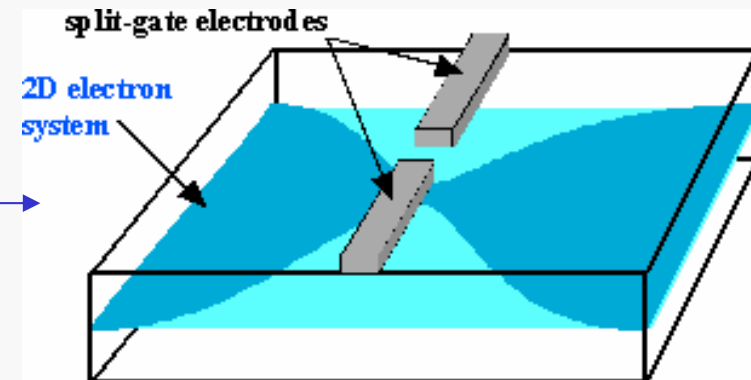
(b) 2-DEG channel formed in the 2-DEG at an AlGaAs/GaAs heterostructure by the action of two evaporated metal gates. If biased negatively they repel the electrons in the 2-DEG below.

(c) A similar effect on the electron concentration in the 2-DEG is obtained by spatially varying ionized donor concentration (positive charges) in the upper AlGaAs layer.



## Split-gate MODFET

(MODulation Doping)



An additional pair of electrodes with a nanosized gap leads to a 1-D like conducting channel

# A closer look at the de Broglie wavelength

## Degenerate and non-degenerate conductors

At equilibrium the available states in a conductor are filled up according to the Fermi function

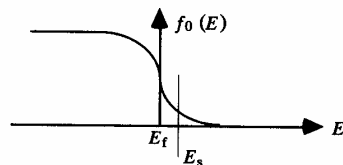
$$f_0(E) = \frac{1}{1 + \exp[(E - E_f)/k_B T]} \quad (1.2.7)$$

where  $E_f$  is the Fermi energy. Away from equilibrium the system has no common Fermi energy, but often we can talk in terms of a local quasi-Fermi level which can vary spatially and which can be different for different groups of states (such as electrons and holes) even at the same spatial location. We will generally use  $F_n$  to denote quasi-Fermi levels and reserve  $E_f$  for the equilibrium Fermi energy.

There are two limits in which the Fermi function inside the band ( $E > E_s$ ) can be simplified somewhat making it easier to perform numerical calculations (see Fig. 1.2.2). One is the high temperature or the non-degenerate limit ( $\exp[E_s - E_f]/k_B T \gg 1$ ) where

$$f_0(E) \approx \exp[-(E - E_f)/k_B T] \quad (1.2.8)$$

(a) Non-degenerate limit



(b) Degenerate limit

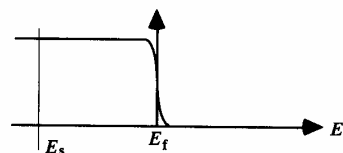


Fig. 1.2.2. The Fermi function inside the band ( $E > E_s$ ) can be approximated by (a) Eq.(1.2.8) in the non-degenerate limit and (b) by Eq.(1.2.9) in the degenerate limit.

The other is the low temperature or the degenerate limit ( $\exp[E_s - E_f]/k_B T \ll 1$ ) where

$$f_0(E) \approx \vartheta(E_f - E) \quad (1.2.9)$$

In this book we will mainly be discussing degenerate conductors.

To relate the equilibrium electron density  $n_s$  (per unit area) to the Fermi energy we make use of the relation

$$n_s = \int N(E) f_0(E) dE$$

For degenerate conductors it is easy to perform the integral to obtain

$$n_s = N_s (E_f - E_s) \quad \text{where} \quad N_s = m/\pi \hbar^2 \quad (1.2.10)$$

where we have made use of Eqs.(1.2.6) and (1.2.9).

At low temperatures the conductance is determined entirely by electrons with energy close to the Fermi energy. The wavenumber of such electrons is referred to as the Fermi wavenumber ( $k_f$ ):

$$E_f - E_s = \frac{\hbar^2 k_f^2}{2m} \Rightarrow \hbar k_f = \sqrt{2m(E_f - E_s)} \quad (1.2.11)$$

Using Eq.(1.2.10) we can express the Fermi wavenumber in terms of the electron density:

$$k_f = \sqrt{2\pi n_s} \quad (1.2.12)$$

The corresponding velocity is the Fermi velocity  $v_f = \hbar k_f/m$ .

**In the “degenerate case” (low temperature) Fermi velocity depends on the square root of the electron density**

# Criteria for 1DEG situations

## 1.3 Characteristic lengths

A conductor usually shows ohmic behavior if its dimensions are much larger than certain characteristic lengths, namely, (1) the de Broglie wavelength, (2) the mean free path, and (3) the phase-relaxation length. We will discuss these one by one. In addition to these characteristic lengths, the screening length can also play a significant role especially in low-dimensional conductors as we will see in Section 2.3 (see Fig. 2.3.3).

### Wavelength ( $\lambda$ )

We have seen (Eq.(1.2.12)) that the Fermi wavenumber  $k_f$  goes up as the square root of the electron density. The corresponding wavelength goes down as the square root of the electron density:

$$\lambda_f = 2\pi/k_f = \sqrt{2\pi/n_s}$$

**De Broglie wavelength at the Fermi velocity**

For an electron density of  $5 \times 10^{11}/\text{cm}^2$ , the Fermi wavelength is about 35 nm. At low temperatures the current is carried mainly by electrons having an energy close to the Fermi energy so that the Fermi wavelength is the relevant length. Other electrons with less kinetic energy have longer wavelengths but they do not contribute to the conductance.

### Mean free path ( $L_m$ )

An electron in a perfect crystal moves as if it were in vacuum but with a different mass. Any deviation from perfect crystallinity such as impurities, lattice vibrations (phonons) or other electrons leads to 'collisions' that scatter the electron from one state to another thereby changing its momentum. The momentum relaxation time  $\tau_m$  is related to the collision time  $\tau_c$  by a relation of the form

$$\frac{1}{\tau_m} \rightarrow \frac{1}{\tau_c} \alpha_m$$

where the factor  $\alpha_m$  (lying between 0 and 1) denotes the 'effectiveness' of an individual collision in destroying momentum. For example if the

collisions are such that the electrons are scattered only by a small angle then very little momentum is lost in an individual collision. The factor  $\alpha_m$  is then very small so that the momentum relaxation time is much longer than the collision time. For a more detailed discussion of scattering times in semiconductors see, for example, Chapter 4 of S. Datta (1989), *Quantum Phenomena*, Modular Series on Solid-state Devices, vol. VIII, eds. R. F. Pierret and G. W. Neudeck, (New York, Addison-Wesley).

The mean free path,  $L_m$ , is the distance that an electron travels before its initial momentum is destroyed; that is,

$$L_m = v_f \tau_m \tag{1.3.2}$$

where  $\tau_m$  is the momentum relaxation time and  $v_f$  is the Fermi velocity. The Fermi velocity is given by

$$v_f = \frac{\hbar k_f}{m} = \frac{\hbar}{m} \sqrt{2\pi n_s} \rightarrow 3 \times 10^7 \text{ cm/s} \quad \text{if } n_s = 5 \times 10^{11} / \text{cm}^2$$

Assuming a momentum relaxation time of 100 ps we obtain a mean free path of  $L_m = 30 \mu\text{m}$ .

### Phase-relaxation length ( $L_\phi$ )

Let us first discuss what is meant by the phase-relaxation time ( $\tau_\phi$ ). We will then relate it to the phase-relaxation length. In analogy with the momentum relaxation time we could write

$$\frac{1}{\tau_\phi} \rightarrow \frac{1}{\tau_c} \alpha_\phi$$

where the factor  $\alpha_\phi$  denotes the effectiveness of an individual collision in destroying phase. The destruction of phase is, however, a little more subtle than the destruction of momentum. A more careful discussion is required to define what the effectiveness factor  $\alpha_\phi$  is for different types of scattering processes.

# A rough picture of 1DEG conductivity

In the bulk, classically we have:

$$\mathbf{J} = n e \mathbf{v}$$

1. At  $T=0$  only the portion of electrons  $eV/E_F$  is involved in the transport process

2. Fermi velocity must be considered:

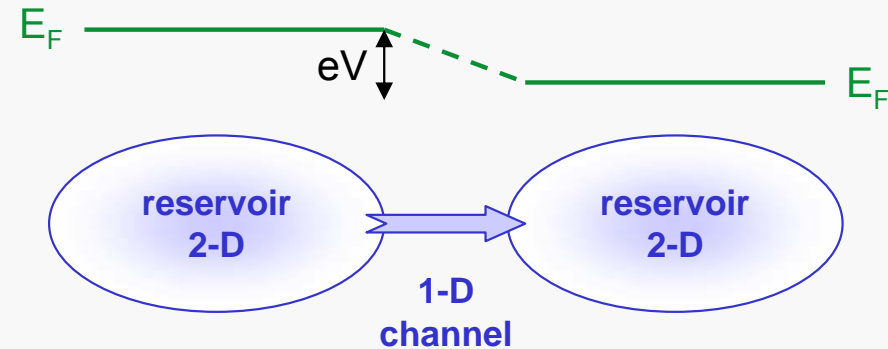
$$v_F = \sqrt{2E_F/m};$$

3.  $n \propto \int g(E)dE$ ; in the 1-D case  $\propto \sqrt{E_F}$

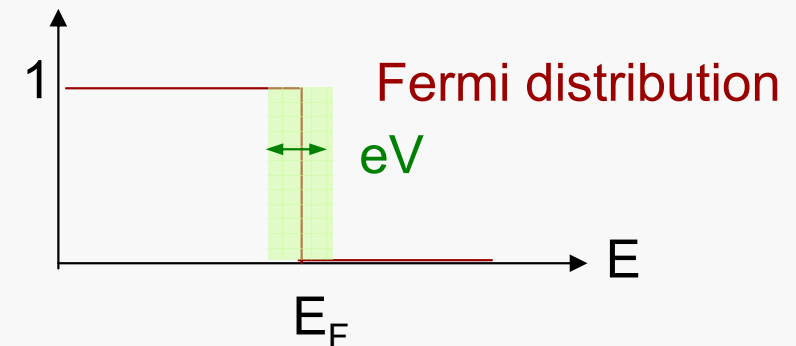
$$I = eV/E_F e \sqrt{2E_F/m} \sqrt{2m E_F}/h = 2 e^2 V/h$$

Conductivity in an ideal 1DEG structure:

$$G_{1D} = i/V = 2 e^2/h$$



Mean occupation number



**1DEG DOS peculiarities lead to a quantized conductivity**

# Landauer levels (intrawire tunneling)

“tunneling” through a quantum wire

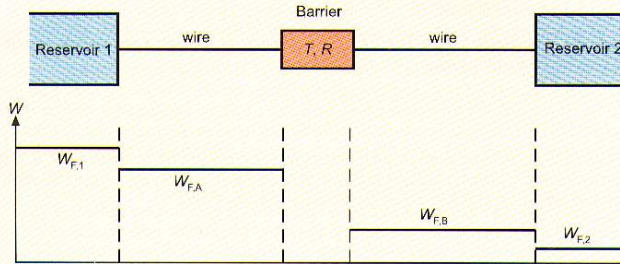


Figure 19: One-channel model for the derivation of ballistic quantum transport through a barrier between two reservoirs. The barrier is described by its transmittance  $T$  and its reflectance  $R$ .  $\mu_1$ ,  $\mu_2$ ,  $\mu_A$  and  $\mu_B$  are the chemical potentials in the different regions.

A general description of non-diffusive quantum-mechanical transport in nano- and mesoscopic structures has been developed by Landauer [9] and Büttiker [10]. In the idealized model two reservoirs 1 and 2 characterized by their chemical potentials  $W_{F,1}$  and  $W_{F,2}$  are connected through two ideal 1-D wires of length  $L$ . In these wires the electronic states are plane waves  $\psi(x) = \exp(ikx)/\sqrt{L}$ , which can have positive and negative  $k$ -vectors and two spin orientations. With the quantum-mechanical expression for the current density in one dimension

$$j = \frac{e\hbar}{2im} (\psi^* \nabla \psi - \psi \nabla \psi^*) \quad \text{(quantum) current density} \quad (55)$$

the corresponding current for one  $k$ -vector and one spin orientation is obtained as

$$I = \frac{e\hbar k}{mL} \quad (56)$$

Between the two wires an energetic barrier for the electrons is assumed, which is characterized by its quantum-mechanical reflection coefficient  $R$  and its transmission coefficient  $T$ , with  $T + R = 1$  (Figure 19).

Due to the difference  $W_{F,1} - W_{F,2}$  of the chemical potentials a current through the wires is induced. It results from electrons with energies  $W_{F,1} \geq W \geq W_{F,2}$  and  $k$ -vectors in positive forward direction, which occupy the electronic states in the left wire. Part of the current is reflected at the barrier and the other part is transmitted. The reflected current is absorbed in reservoir 1 while the transmitted part is absorbed in reservoir 2. Only within these reservoirs does energy dissipation occur. The total current in the positive  $k$ -direction in the left wire is thus obtained by adding up all occupied states and using (56) as

$$I_{\leftarrow} = \frac{e\hbar k}{mL} LD^{(1)}(W)(W_{F,1} - W_{F,2}) \quad (57)$$

$D^{(1)}(W)$  is the 1-D density of states (per wire length  $L$ ) according to (51). With  $W = \hbar^2 k^2 / 2m$  this yields

$$I_{\leftarrow} = \frac{e}{\pi\hbar} (W_{F,1} - W_{F,2}) \quad (58)$$

and for the transmitted net current in the right wire

$$I = \frac{e}{\pi\hbar} T (W_{F,1} - W_{F,2}) \quad (59)$$

The reflected current  $I_R$  in the left wire is accordingly

$$I_R = \frac{e}{\pi\hbar} R (W_{F,1} - W_{F,2}) \quad (60)$$

For the determination of the chemical potentials the total number of states in the wires, with positive and negative  $k$ -values, has to be taken into account, i.e.  $2D^{(1)}(W)(W_{F,1} - W_{F,2})$ . In the right wire the current, which is induced by  $(W_{F,1} - W_{F,2})$ , corresponds to a complete occupation of states between  $W_{F,B}$  and  $W_{F,2}$  (Figure 19), such that

$$ID^{(1)}(W)(W_{F,1} - W_{F,2}) = 2D^{(1)}(W)(W_{F,1} - W_{F,2}) \quad (61)$$

Within the left wire both the currents  $I_{\leftarrow}$  and  $I_R$  have to be considered and the resulting occupation of states is assumed to correspond to the occupation of states between  $W_{F,A}$  and  $W_{F,2}$ , such that

$$(1 + R)D^{(1)}(W)(W_{F,1} - W_{F,2}) = 2D^{(1)}(W)(W_{F,A} - W_{F,2}) \quad (62)$$

With  $R + T = 1$  the difference between (61) and (62) yields

$$W_{F,A} - W_{F,B} = R(W_{F,1} - W_{F,2}) \quad (63)$$

With  $V$  as the voltage between both wires and  $eV = W_{F,A} - W_{F,B}$  one obtains from (59) and (63) for the current through the wires

$$I = \frac{e^2}{\pi\hbar} \frac{T}{R} V = \frac{2e^2}{h} \frac{T}{R} V \quad (64)$$

This is the analogue to Ohm's law for quantum transport through a nanoscopic system. The conductance of the system thus follows as

$$G = \frac{2e^2}{h} \frac{T}{R} \quad (65)$$

This so-called Landauer formula again contains the conductivity quantum  $e^2/h$  of 1-D quantum transport. The Landauer formalism for quantum transport can be generalized to a network where several wires connect a barrier with reservoirs.

Da R. Waser Ed., Nanoelectronics and information technology (Wiley-VCH, 2003)

# Ballistic transport

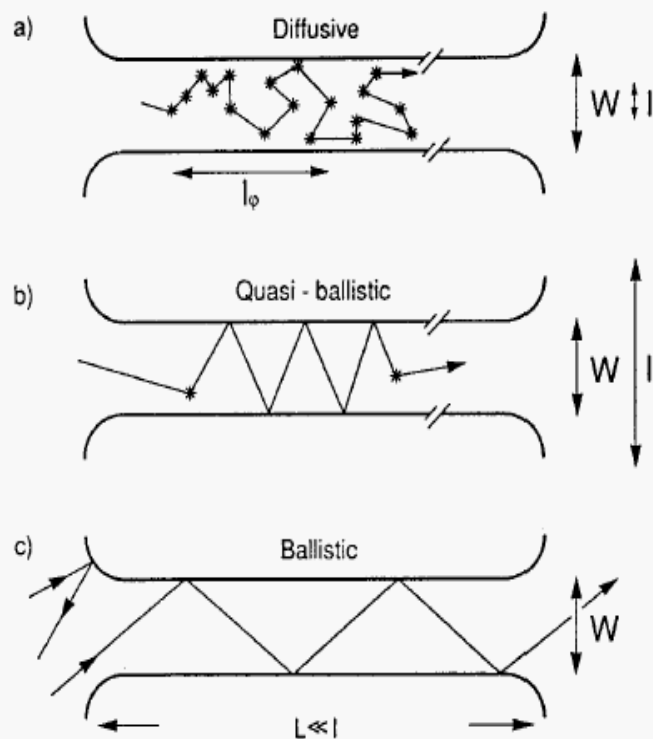


Figure 10.4: Electron trajectories characteristic of the diffusive ( $l < W, L$ ), quasi-ballistic ( $W < l < L$ ), and ballistic ( $W, L < l$ ) transport regimes, for the case of specular boundary scattering. Boundary scattering and internal impurity scattering (asterisks) are of equal importance in the quasi-ballistic regime. A nonzero resistance in the ballistic regime results from backscattering at the connection between the narrow channel and the wide 2DEG regions. Taken from H. Van Houten et al. in "Physics and Technology of Submicron Structures" (H. Heinrich, G. Bauer and F. Kuchar, eds.) Springer, Berlin, 1988.

In the ballistic transport regime, electrons are assumed to move within the structure without scattering (but that at the interface with the ohmic contacts, i.e., the higher-dimensional "outer world")

Behavior analogous to an optical fiber in the total reflection mode

If a quantum wire is considered, comparison between the de Broglie wavelength and the *transverse* size suggests to consider *single mode fibers*

↓  
**Transverse modes**

# Transverse modes I

## 1.6 Transverse modes (or magneto-electric subbands)

In this section we will discuss the concept of transverse modes or subbands which will appear repeatedly in this book. These are analogous to transverse modes (TE<sub>10</sub>, TM<sub>11</sub>, etc.) of electromagnetic waveguides. In narrow conductors, the different transverse modes are well separated in energy and such conductors are often called *electron waveguides*.

We consider a rectangular conductor that is uniform in the  $x$ -direction and has some transverse confining potential  $U(y)$  (see Fig. 1.6.1). The motion of electrons in such a conductor is described by the effective mass equation (see Eq.(1.2.2))

$$\left[ E_s + \frac{(\mathbf{i}\hbar\nabla + e\mathbf{A})^2}{2m} + U(y) \right] \Psi(x, y) = E\Psi(x, y)$$

We assume a constant magnetic field  $B$  in the  $z$ -direction perpendicular to the plane of the conductor. This can be represented by a vector potential of the form

$$\mathbf{A} = -\hat{x}By \Rightarrow A_x = -By \text{ and } A_y = 0$$

so that Eq.(1.2.2) can be rewritten as

$$\left[ E_s + \frac{(p_x + eBy)^2}{2m} + \frac{p_y^2}{2m} + U(y) \right] \Psi(x, y) = E\Psi(x, y) \quad (1.6.1)$$

where 
$$p_x = -i\hbar \frac{\partial}{\partial x} \text{ and } p_y = -i\hbar \frac{\partial}{\partial y}$$

The solutions to Eq.(1.6.1) can be expressed in the form of plane waves ( $L$ : length of conductor over which the wavefunctions are normalized)

$$\Psi(x, y) = \frac{1}{\sqrt{L}} \exp[ikx] \chi(y) \quad (1.6.2)$$

where the transverse function  $\chi(y)$  satisfies the equation

$$\left[ E_s + \frac{(\hbar k + eBy)^2}{2m} + \frac{p_y^2}{2m} + U(y) \right] \chi(y) = E\chi(y) \quad (1.6.3)$$

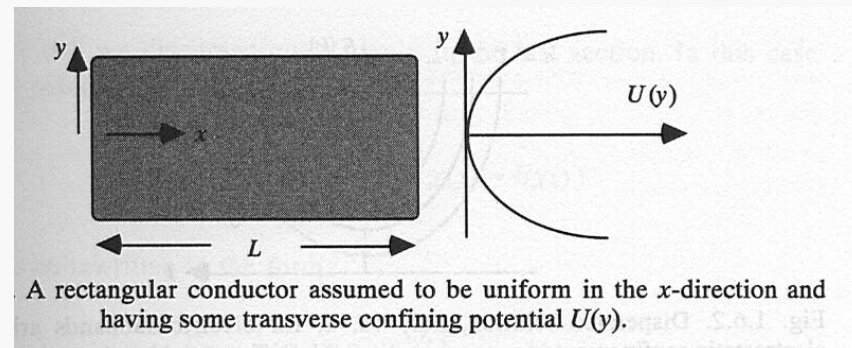
Note that the choice of vector potential is not unique for the given magnetic field. For example we could choose  $A_x = 0$  and  $A_y = -Bx$ . The solutions would then look very different though the physics of course must remain the same. It is only with our choice of gauge, that the solutions have the form of plane waves in the  $x$ -direction. We will use this gauge in all our discussions.

We are interested in the nature of the transverse eigenfunctions and the eigenenergies for different combinations of the confining potential  $U$  and the magnetic field  $B$ . In general for arbitrary confinement potentials  $U(y)$

there are no analytical solutions. However, for a parabolic potential (which is often a good description of the actual potential in many electron waveguides)

$$U(y) = \frac{1}{2} m\omega_0^2 y^2$$

**Model  
confining potential**



Electrons are confined within the structure by a suitable potential

The “transverse eigenfunction” (depending on the potential) must obey the boundary conditions

## Transverse modes II

Confined electrons ( $U \neq 0$ ) in zero magnetic field ( $B = 0$ )

Consider first the case of zero magnetic field, so that Eq.(1.6.3) reduces

$$\left[ E_s + \frac{\hbar^2 k^2}{2m} + \frac{p_y^2}{2m} + \frac{1}{2} m \omega_0^2 y^2 \right] \chi(y) = E \chi(y) \quad (1.6.4)$$

The eigenfunctions of Eq.(1.6.4) are well-known (see any quantum mechanics text such as L. I. Schiff (1968), *Quantum Mechanics*, Third Edition, (New York, McGraw-Hill) Section 13). The eigenenergies and eigenfunctions are given by

$$\chi_{n,k}(y) = u_n(q) \quad \text{where} \quad q = \sqrt{m\omega_0/\hbar} y \quad (1.6.5a)$$

$$E(n, k) = E_s + \frac{\hbar^2 k^2}{2m} + (n + \frac{1}{2})\hbar\omega_0, \quad n = 0, 1, 2, \dots \quad (1.6.5b)$$

### Subbands

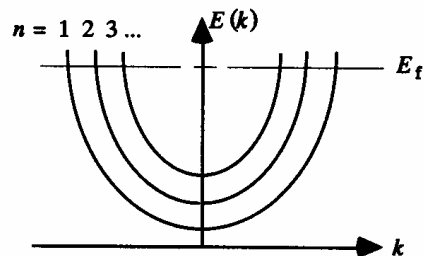


Fig. 1.6.2. Dispersion relation,  $E(k)$  vs.  $k$ , for electric subbands arising from electrostatic confinement in zero magnetic field. Different subbands are indexed by  $n$ .

After S.Datta, *Electronic Transport in Mesoscopic Systems*, Cambridge (1997)

where

$$u_n(q) = \exp[-q^2/2] H_n(q)$$

$H_n(q)$  being the  $n$ th Hermite polynomial. The first three of these polynomials are

$$H_0(q) = \frac{1}{\pi^{1/4}}, \quad H_1(q) = \frac{\sqrt{2}q}{\pi^{1/4}} \quad \text{and} \quad H_2(q) = \frac{2q^2 - 1}{\sqrt{2}\pi^{1/4}}$$

The velocity is obtained from the slope of the dispersion curve:

$$v(n, k) = \frac{1}{\hbar} \frac{\partial E(n, k)}{\partial k} = \frac{\hbar k}{m} \quad \text{Group velocity} \quad (1.6.5c)$$

The dispersion relation is sketched in Fig. 1.6.2. States with different index  $n$  are said to belong to different subbands just like the subbands that arise from the confinement in the  $z$ -direction (see Section 1.2). The spacing between two subbands is equal to  $\hbar\omega_0$ . The tighter the confinement, the larger  $\omega_0$  is, and the further apart the subbands are. Usually the confinement in the  $z$ -direction is very tight ( $\sim 5$ – $10$  nm) so that the corresponding subband spacing is large ( $\sim 100$  meV) and only one or two subbands are customarily occupied. Indeed, in all our discussions we will assume that only one  $z$ -subband is occupied. But the  $y$ -confinement is relatively weak and the corresponding subband spacing is often quite small so that a number of these are occupied under normal operating conditions. The subbands are often referred to as *transverse modes* in analogy with the modes of an electromagnetic waveguide.

**Quantization (subbands) arises when solving the Schroedinger equation in the confining potential (transverse modes)**

# Transverse modes III

## Calculating the current

To calculate the current we note that the states in the narrow conductor belong to different transverse modes or subbands as discussed in Section 1.6. Each mode has a dispersion relation  $E(N, k)$  as sketched in Fig. 2.1.1b with a cut-off energy

$$\varepsilon_N = E(N, k = 0)$$

below which it cannot propagate. The number of transverse modes at an energy  $E$  is obtained by counting the number of modes having cut-off energies smaller than  $E$ :

$$M(E) = \sum_N \vartheta(E - \varepsilon_N) \quad (2.1.1)$$

We can evaluate the current carried by each transverse mode (numbered by 'N' in Fig. 2.1.1b) separately and add them up.

Consider a single transverse mode whose  $+k$  states are occupied according to some function  $f^+(E)$ . A uniform electron gas with  $n$  electrons per unit length moving with a velocity  $v$  carries a current equal to  $env$ . Since the electron density associated with a single  $k$ -state in a conductor of length  $L$  is  $(1/L)$  we can write the current  $I^+$  carried by the  $+k$  states as

$$I^+ = \frac{e}{L} \sum_k v f^+(E) = \frac{e}{L} \sum_k \frac{1}{\hbar} \frac{\partial E}{\partial k} f^+(E)$$

Assuming periodic boundary conditions (see Fig. 1.2.1 and related discussion) and converting the sum over  $k$  into an integral according to the usual prescription

$$\sum_k \rightarrow 2 \text{ (for spin)} \times \frac{L}{2\pi} \int dk$$

we obtain

$$I^+ = \frac{2e}{h} \int_{\varepsilon}^{\infty} f^+(E) dE$$

where  $\varepsilon$  is the cut-off energy of the waveguide mode. We could extend this result to multi-moded waveguides and write the current,  $I^+$ , carried by the  $+k$  states in a conductor as

$$I^+ = \frac{2e}{h} \int_{\varepsilon}^{\infty} f^+(E) M(E) dE \quad (2.1.2)$$

where the function  $M(E)$  (defined in Eq.(2.1.1)) tells us the number of modes that are above cut-off at energy  $E$ . Note that this is a general result independent of the actual dispersion relation  $E(k)$  of the waveguide: the current carried per mode per unit energy by an occupied state is equal to  $2|e|/h$  (which is about 80 nA/meV).

## Contact resistance

Assuming that the number of modes  $M$  is constant over the energy range  $\mu_1 > E > \mu_2$ , we can write

$$I = \frac{2e^2}{h} M \frac{(\mu_1 - \mu_2)}{e} \Rightarrow G_c = \frac{2e^2}{h} M \quad (2.1.3)$$

so that the contact resistance (which is the resistance of a ballistic waveguide) is given by

$$G_c^{-1} = \frac{(\mu_1 - \mu_2)e}{I} = \frac{h}{2e^2 M} \approx \frac{12.9 \text{ k}\Omega}{M}$$

Note that the contact resistance goes down inversely with the number of modes. The contact resistance of a single-moded conductor is  $\sim 12.9 \text{ k}\Omega$ , which is certainly not negligible! This is the resistance one would measure if a single-moded ballistic conductor were sandwiched between two conductive contacts.

Usually we are concerned with wide conductors having thousands of modes so that the contact resistance is very small and tends to go unnoticed. To calculate the number of modes  $M(E)$  we need to know the cut-off energies for the different modes  $\varepsilon_N$ . As we have seen in Section 1.6, the details depend on the confining potential  $U(y)$  and the magnetic field. However, for wide conductors in zero magnetic field the precise nature of the confining potential is not important. We can estimate the number of modes simply by assuming periodic boundary conditions. The allowed values of  $k_y$  are then spaced by  $2\pi/W$  (see Fig. 1.2.1), with each value of  $k_y$  corresponding to a distinct transverse mode. At an energy  $E_t$  ( $= \hbar^2 k_t^2 / 2m$ ), a mode can propagate only if  $-k_t < k_y < k_t$ . Hence the number of propagating modes can be written as

$$M = \text{Int} \left[ \frac{k_t W}{\pi} \right] = \text{Int} \left[ \frac{W}{\lambda_t / 2} \right]$$

where  $\text{Int}(x)$  represents the integer that is just smaller than  $x$ . Assuming a Fermi wavelength of 30 nm, the number of modes in a 15  $\mu\text{m}$  wide field-effect transistor is approximately 1000, so that the contact resistance is about 12.5  $\Omega$ .

**The waveguide supports transverse modes below some (energy) cut-off, leading to Landauer levels**

## SPLIT GATE

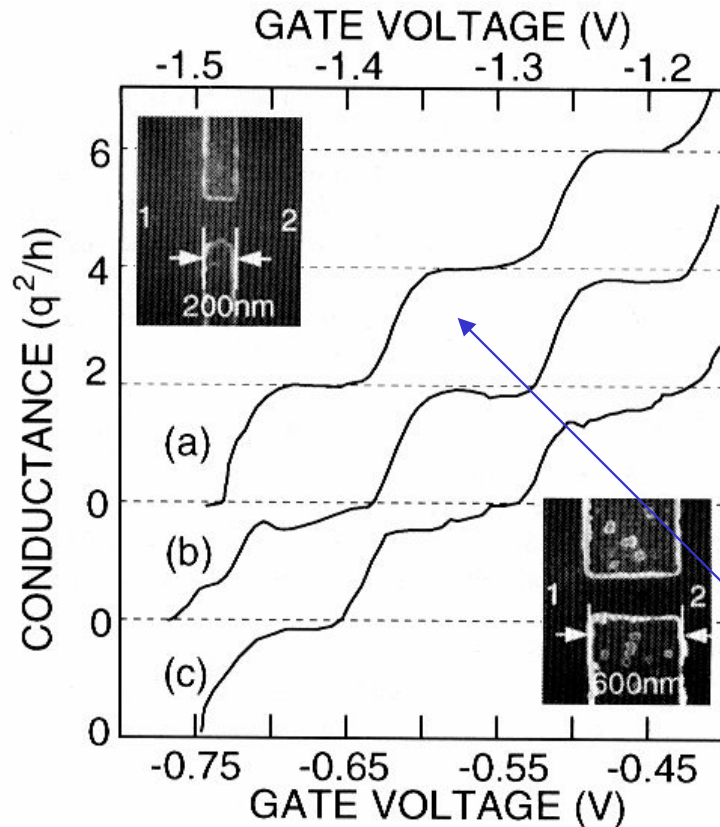


**FIGURE 19.** The two terminal conductance of an electron waveguide at  $T=280\text{mK}$  as a function of gate voltage (or the width of the constriction). The inset at the top of the figure shows a top view of 200 nm long split-gate electrodes with a 300 nm gap between them placed on a high mobility  $GaAs/AlGaAs$  heterostructure. The bottom inset shows a similar device on the same heterostructure with a 600 nm lithographic length. The quantization of the conductance ( $\delta G = (1 \pm 0.01) 2q^2/h$ ) of the 200 nm long constriction shown in (a) deteriorates after cycling to room temperature, as shown in (b). We attribute the deterioration to a difference in the configuration of depletion charges corresponding variations in the width of the constriction. The poor quantization of the conductance of a 600 nm long constriction, shown in (c), is also supposed to develop from fluctuations in the width. (See color plate.)

## POINT CONTACT

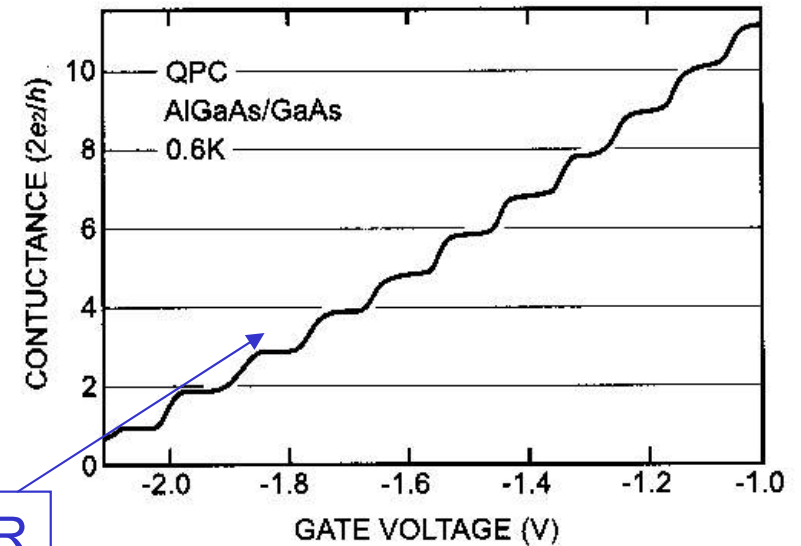


**Figure 18:** Quantized conductance of a quantum point contact (QPC) at 0.6K prepared at a  $AlGaAs/GaAs$  interface (2-DEG). The conductance was obtained from the measured resistance after subtraction of a constant series resistance of  $400 \Omega$  (After [8]).

LANDAUER  
LEVELS

**Quantized resistance  
observed (at very low T)**

# Electron waveguides II

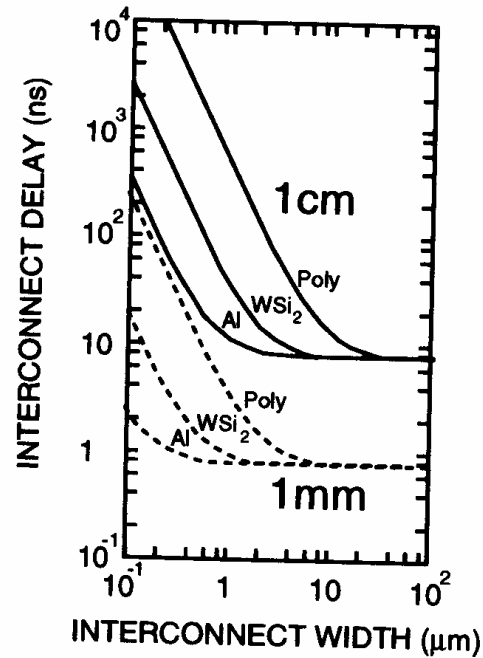
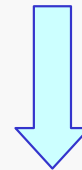


**FIGURE 15.** The interconnection delay for 1 cm and 1 mm long lines as a function of line width for three materials Al, WSi<sub>2</sub>, and polysilicon assuming a channel resistance of  $R_{ch} \approx 1 k\Omega$ . It is assumed that the spacing between lines is equal to the width, that the interconnection thickness is a third of the width, and that the dielectric thickness is about a fifth of the width. Constant field scaling is applied and we assume that  $\rho_{Al} = 3 \mu\Omega\text{cm}$ ,  $\rho_{WSi_2} = 30 \mu\Omega\text{cm}$ , and  $\rho_{Poly} = 500 \mu\Omega\text{cm}$ , for the respective resistivities. Adapted from Bakoglu[95].

If conductance is not affected by diffusive transport:

- resistance (within the wire) is negligible;
- speed is at a maximum;
- dissipation can be neglected;
- *single electron transport* can be achieved (no doubt a *single* charge entering the structure is transmitted!)



Quantum wire potentially suitable as unconventional interconnects  
(but cumbersome fabrication, need to operate at very low T!)

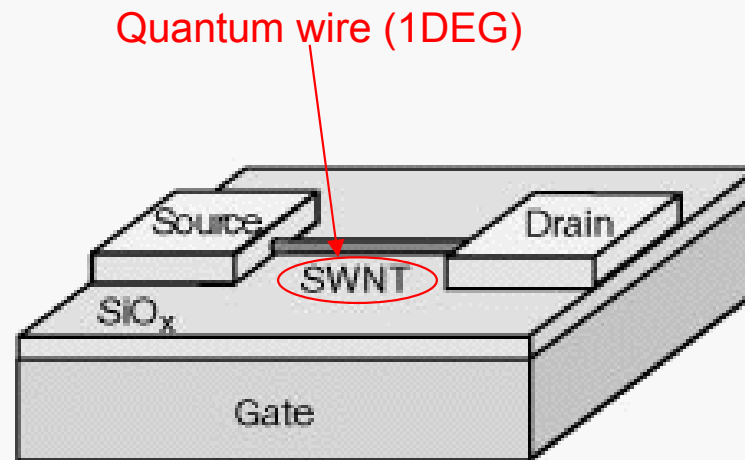
# 1DEG and active devices?

Can the 1DEG transport properties be exploited in a three-terminal (active) device?

Can a 1DEG-channel MOSFET (not just a split-gate) be realized?

[The idea is to control the few/single electron flow across the wire with an additional electric field or voltage]

We will see in “non conventional” implementations!  
(possibly with less fabrication problems)



# Conclusions

- ✓ Transport properties (conductivity) is strongly affected by dimensionality
- ✓ Lower dimensionality implies a different functional dependence of DOS on the energy
- ✓ Quantum confinement effects may arise when considering nanostructures with size comparable to the de Broglie wavelength (either single-particle, or degenerate semiconductors)
- ✓ Quantum Hall Effect (2DEG + magnetic field) demonstrates quantized resistance
- ✓ Similar quantization effects (but for factor 2!) is observed also in electron waveguides
- ✓ Landauer levels can be associated to transverse modes